Vegetation History and Archaeobotany (2025) 34:239–255
https://doi.org/10.1007/s00334-024-01012-9

ORIGINAL ARTICLE

Predicting plant water availability from phytolith assemblages: an experimental approach for archaeological reconstructions in drylands

Francesca D'Agostini[1,2] · Javier Ruiz Pérez[1] · Marco Madella[1,3,4] · Vincent Vadez[2,5] · Carla Lancelotti[1,3]

Received: 4 December 2023 / Accepted: 11 April 2024 / Published online: 7 November 2024

Abstract

In this study we investigate the relationship between phytolith formation and transpiration rate in *Eleusine coracana* (finger millet), *Cenchrus americanus* (syn. *Pennisetum glaucum*, pearl millet) and *Sorghum bicolor* (sorghum). The aim is to produce a prediction model to reconstruct water management for agriculture in archaeological contexts in drylands. Two kinds of phytolith proxy evidence have been tested in modern experimental growing seasons as indicators of water availability, the ratio of sensitive to fixed morphotypes and also a logistic regression predictive model built on the complete assemblage of all morphotypes of the three species. Our results show a relationship between total water transpired and phytolith formation, which can be best predicted by the application of statistical logistic regressions. This is because some morphotypes are positively correlated with water availability, others are negatively correlated, and the significance of specific morphotypes in response to water availability varies according to the species and the part of the plant where the phytolith is formed. Indeed, water stress prompts each plant to alter its phytolith production in a distinct manner. The outcomes of this investigation should be of interest to archaeobotanists seeking a way of detecting the past growing conditions of C_4 crops, but also to physiologists and ecologists who are interested in the study of phytolith formation.

Keywords Phytoliths · Water availability · Agriculture · Sorghum · Pearl millet · Finger millet

Introduction

Today, dry lands cover over 40% of the Earth's surface and are home to approximately 2.3 billion people (International Institute for Environment and Development 2022). Arid and hyper-arid dry lands have often been considered peripheral regions, posing a challenge for human settlement and agriculture both in the present and in the past (Biagetti et al. 2021). At the same time, anthropological and archaeological research has shown that traditional socio-ecological systems in dry lands are very resilient and highly adaptive (Critchley and Gowing 2012; D'Odorico and Bhattachan 2012; Balbo et al. 2016). Various practices have been adopted in dry areas to manage water resources by collecting rain and groundwater, channelling floodwater and carefully using the few water resources available, especially for farming (Prinz 2002; Marshall and Weissbrod 2011; Manning and Timpson 2014). Archaeological and historical data has confirmed that these are the areas where the domestication of various crops first began (Manning et al. 2011; Winchell et al. 2018) and also where the technologies that supported sophisticated agricultural systems first occurred (Winslow et al. 2004; Reynolds et al. 2007). However, the study of the long-term dynamics of these practices has been hampered by the scarcity of reliable archaeological proxy evidence for water availability to plants.

Communicated by R.M. Albert.

✉ Francesca D'Agostini
francesca.dagostini@upf.edu

[1] CASEs Research Group, Department of Humanities, University Pompeu Fabra, c/ Ramon Trias Fargas 25-27, Barcelona 08005, Spain

[2] University of Montpellier, IRD (Institut de Recherche pour le Développement), DIADE Unit, Av. Agropolis 911, Montpellier 34394, France

[3] ICREA, Pg. Lluís Companys 23, Barcelona 08010, Spain

[4] School of Geography, Archaeology and Environmental Studies, University of Witwatersrand, 1 Jan Smuts Avenue, Braamfontein, Johannesburg 2000, South Africa

[5] Crop Physiology Laboratory, ICRISAT, Patancheruvu, Telangana 502324, India

The main aim of the present study is to explore the reliable use of phytolith data to directly assess past water availability for dry land farming. Phytoliths are one of the several proxies in the archaeological record that have been used to understand the presence and use of water (Madella et al. 2009). Other available options for this purpose are direct proxies such as stable carbon isotopes in seeds, as well as indirect proxies which include artificial structures such as wells, canals or water tanks that indicate some sort of water management system (Prinz 2002).

Most of the archaeobotanical research to assess the availability of water to crops has so far focused on C_3 plants such as *Triticum* (wheat), *Hordeum* (barley) and *Oryza* (rice), which are some of the main crops of both modern and ancient agriculture in some of the most studied areas of the world (for example, Jenkins et al. 2016), and because their physiological processes in relation to water supply are less complex than in C_4 plants (Sage 2004), which include some millets and *Sorghum bicolor* (sorghum). The study of the stable carbon isotope composition of C_3 grains has long been considered an efficient indicator of water availability (Araus et al. 1997; Ferrio et al. 2005; Nitsch et al. 2015). However, some of the most important traditional crops grown in dry lands have a C_4 carbon fixation pathway that is better adapted to drought but much more complex, both anatomically and physiologically. Indeed, the exact relationship between water availability and C_4 carbon discrimination still needs to be clarified. In addition, the taxonomic identification of C_4 grains from archaeological assemblages is further complicated because most of them, such as *Eleusine coracana* (finger millet) and *Cenchrus americanus* (pearl millet) produce very small grains that are highly affected by charring and post depositional taphonomy (Weber and Fuller 2008). The relationship between taphonomic effects and C_4 carbon discrimination have only recently begun to be studied (Yang et al. 2011; Beldados and Ruiz-Giralt 2023; Varalli et al. 2023).

Phytoliths, being inorganic, are much less affected by pre- and post-depositional processes than cereal grains and other plant remains (Piperno 2006). Researchers have been proposing phytoliths as a proxy for water availability since the early 1990s. Rosen and Weiner (1994) first suggested using the size of silica skeletons (epidermal sheets), under the assumption that higher water absorption by the plant leads to a greater silica uptake, which in turn causes the formation of larger silica skeletons. This methodology has been applied by Katz et al. (2007), who used the number of ELONGATE morphotypes in silica skeletons from household contexts to infer dry farming in the southern Levant during the Chalcolithic (4400 – 4300 BCE). However, mechanical pressure (Madella and Lancelotti 2012) or even phytolith extraction methods (Jenkins 2009) can cause cell disarticulation and compromise silica skeleton size. Bremond et al. (2005) suggested a humidity-aridity index (Iph %) based on the abundance of fan-shaped BULLIFORM (BULLIFORM FLABELLATE) in Chloridoideae phytolith assemblages for climatic/vegetation reconstruction, hypothesising that the more the plant transpires and/or suffers water stress, the more silicified bulliform cells would be produced. Madella et al. (2009) proposed the use of a ratio of fixed morphotypes (genetically determined, mainly short cells) to sensitive morphotypes (environmentally controlled ones, mainly ELONGATE and STOMA). This approach was validated in experimentally grown *Triticum aestivum* L. (bread wheat), *Triticum dicoccum* L. (emmer wheat) and *Hordeum vulgare* L. (barley). The methodology was then applied by Weisskopf et al. (2015) to detect water availability in fields of *Oryza sativa* (rice), and by Jenkins et al. (2016) who also grew barley and *Triticum durum* Desf. (durum wheat) experimentally. These studies showed higher ratios in irrigated crops in comparison to non irrigated (rainfed) ones. More recently, Jenkins et al. (2020) and Ermish and Boomgarden (2022) suggested applying the same ratio to C_4 crops, namely *Sorghum bicolor* (L.) Moench (sorghum) and *Zea mays* L. (maize). The results of all these studies produced larger proportions of long cells from irrigated crops compared to the non-irrigated ones, indicating that the methodology is also effective in crops with reduced transpiration and thus biosilica deposition, as is the case of C_4 plants. The first study that analysed more than one species simultaneously is D'Agostini et al. (2023). (*Eleusine coracana* (L.) Gaertn. (finger millet), *Cenchrus americanus* (L.) Morrone syn. *Pennisetum glaucum* (L.) R.Br. (pearl millet) and *Sorghum bicolor* (L.) Moench (sorghum) were experimentally grown and tested for the biosilica production in their leaves in relation to transpiration. BULLIFORM, and to a lesser extent STOMA, proved to be the most effective morphotypes in predicting whether the entire assemblage originated from an irrigated or non-irrigated plant.

These three crops have also been selected in this study, which aims to analyse the data obtained from two seasons of the same experiment, one in 2019 (D'Agostini et al. 2023) and the other in 2020. In doing so, we aim to enhance the robustness of the analysis by using a larger sample size compared to that previously used. Therefore, the reason for the selection of these three species is the same as in the previous study. First, because they are all biosilica accumulators (Lux et al. 2002; Ma and Yamaji 2006; Kumar et al. 2017; Out and Madella 2017; Coskun et al. 2021). Second, they have distinct biochemical C_4 carbon deposition pathways: NADP-ME for sorghum and NAD-ME for finger millet and pearl millet. This anatomical and biochemical diversity allows evaluation of the resulting differences between C_4 sub-types. Third, key information on transpiration rates and

adaptation to water stress is available (for example, Vadez et al. 2011), showing that not all taxa respond similarly to drought. Fourth, the three species that we used are found in the archaeobotanical assemblages from many settlements in arid regions both in Asia and Africa as they have been grown there as crops since farming began, for example evidence of early use of sorghum has been identified at Mezber and Ona Adi (D'Andrea et al. 2015; Ruiz-Giralt et al. 2023b), *Eleusine coracana* at Harappa (Weber and Kashyap 2016) and *Cenchrus* at Kanmer (Pokharia et al. 2014). Furthermore, according to the International Crop Research Institute for the Semi-Arid Tropics (ICRISAT), these three are currently among the widest cultivated millets in eastern and southern Africa as well as in South Asia (Kumar et al. 2023).

The research presented in this paper was motivated by the following objectives:

1. To refine the methodological approach introduced by D'Agostini et al. (2023) by increasing the number of plants from which the experimental data were obtained and with the addition of new phytolith data. These would provide a more accurate model for interpretation of archaeological phytolith assemblages composed of different taxa and plant parts. This study represents a continuation of the one presented in 2023.
2. To further evaluate the ratio between sensitive and fixed morphotypes in C_4 taxa, where previous analyses have shown inconsistent results (D'Agostini et al. 2023).
3. To increase our general understanding of the mechanisms of phytolith deposition. This becomes especially relevant when drawing comparisons among and between particular taxa (Hodson et al. 2005) and when assessing the possible ways in which phytoliths respond to biotic and abiotic stresses like drought (Katz 2019).

Materials and methods

Experimental cultivation

Two experimental cultivations took place at ICRISAT, Hyderabad, India (17°31'N 78°16'E) between February and May 2019 and 2020. The plants were grown in lysimeters, cylindrical soil containers which allow measurement of soil water balance and percolation, simulating real field conditions (Vadez et al. 2011), while allowing measurement of the water transpired by the plant. The amount of transpiration varies according to the adaptations to drought of the taxa or genotypes and provides an indication of the amount of water used by the plant for its growth. The quantity of water received by plants from rainfall or controlled irrigation, on the other hand, is a variable difficult to control because it does not necessarily correlate with the amount of water actually absorbed by the plant, since some of it evaporates, runs off or percolates through the soil to below the root zone (Katz et al. 2013; Jenkins et al. 2020). The lysimeters used in the experiments were 1.50 m long and 30 cm in diameter. Every cylinder was filled with soil from the ICRISAT farm, providing both room for the plants to grow and enough soil volume to replicate field conditions, as in the soil description, below.

Two different water regimes were tested to simulate water availability, first only rain fed (called water stressed, WS) and second irrigated conditions (well watered, WW), which also acted as control. The lysimeters were weighed to calculate plant water loss from transpiration (Vadez et al. 2021) and watered, weekly in 2019 and every two weeks in 2020, due to the COVID-2019 pandemic and the resulting reduction of available staff during active lockdowns. The WW plants were watered to maintain 80% of soil field capacity, which is the optimum for crops well adapted to dry climates (Zaman-Allah et al. 2011). The WS plants were watered to imitate a rain fed environment in arid areas, where water is usually very limited during the main growing season (Portmann et al. 2010). Therefore, WS plants received an average of 11 L of water per cylinder, maintaining the moisture level at 80% of soil field capacity until flowering began, when watering was stopped, causing stress late in the life cycle. The amount of water given to WS plants corresponded roughly to the average quantity of rainfall that plants receive in arid regions (Climate North West Knowledge 2022). This represented a heavy stress for the WS plants, which matured entirely in the absence of water. Raw data for both seasons of the experiment are available as supporting ESM files at (ESM S1). A more detailed description of the experiment is also available in D'Agostini et al. (2022b).

Ten landraces of each species were selected from those available in the ICRISAT gene bank and used for the experimental growings in both 2019 and 2020. These landraces were selected according to the climate of their original growing regions, taking into account the full spectrum of climatic variations in drylands (D'Agostini et al. 2022b, 2023). In each experimental growing, five biological replicates per landrace from each of the three species were grown under both well watered and water stressed conditions, with a total of 300 lysimeter cylinders. The experiments followed a completely randomised block design, with water treatment as the main factor and the various taxa as the sub-factor, which were randomised within each block of WS or WW treatment. The maps of the experimental designs are available in the supporting data (ESM S1).

Temperature and relative humidity were measured every 30 min by two Gemini Tinytag Ultra 2 TGU-4500 data

loggers which were placed among the leaves of the crop and protected by a well-ventilated styrofoam box to avoid direct radiation. In 2019 the average temperature (± standard error) during the growing season was 32.28 ± 0.1 ºC (min 19 ºC, max 50.5 ºC) with relative humidity (± standard error) at 42.57 ± 0.23% RH (min 13.5%, max 87%). In 2020 the average temperature in the season was 28.64 ± 0.52 ºC (min 11.6 ºC, max 42.8 ºC) with relative humidity at 61.7 ± 1.47% RH (min 18%, max 98%). The soil in the lysimeters was a mixture of 1:1 alfisol and vertisol which had been left fallow for about eight months by the time of the first sowing. The soil mix had not been fertilised since 2018, nor was it during the two growing seasons. The elemental composition of the soil was measured in two cylinders of finger millet (WW and WS), two of sorghum (WW and WS) and one of pearl millet (WS), randomly chosen after the 2020 harvest. The soil of a total of 40 samples was analysed, with the sample size for each plant and cylinder chosen to ensure a comprehensive analysis. Finger millet and sorghum cylinders were sampled from the topsoil every 10 cm down to 90 cm, whereas the pearl millet cylinder was only analysed from deeper down, from 60 cm to 90 cm, to understand the silicon component at the root apex level ($n = 9$ samples per cylinder, n x 2 cylinders = 18 for finger millet, n x 2 cylinders = 18 for sorghum, n / 2 (half cylinder) = 4 for pearl millet, in total, 40 soil samples). The soil was analysed for the composition of its elements at the Barcelona Institute of Geosciencies of the Consejo Superior de Investigaciones Científicas (CSIC, Spanish National Research Council) (GEO3BCN-CSIC) using a Bruker Tracer-5 g pXRF spectrometer with mudrock calibration on samples analysed for 120 s. The average soil silicon content (± 1 standard deviation) in cylinders was 10 ± 1% (w/w), min 77% (w/w), max 11% (w/w)) for finger millet; it was 88 ± 3% (w/w) (min 44% (w/w), max 11% (w/w) for pearl millet; and 99 ± 22% (w/w), min 6% (w/w), max 11% (w/w) for sorghum. Based on these results, the silicon content is considered consistent in all the samples. The complete soil analysis data are in ESM S1.

The WW plants were harvested when the panicles reached maturity after a complete lifecycle. To prevent the WS plants from drying out completely, we harvested them when their transpiration rate dropped below 10% of the value of WW plants, indicating full stomatal closure and intense water-stress imposition, and that any further water loss was through the cuticle (Schuster et al. 2017).

Phytolith extraction, counting and classification

The leaves and chaff from the plants were analysed as they produce most of the phytoliths with taxonomic significance and also morphotypes from cells directly related to transpiration such as Stoma and Bulliform. Leaves of the plants grown in 2019 were analysed in bulk (D'Agostini et al. 2023) while in the 2020 crop the top five leaves were analysed separately from the others (Table 1). The top five leaves are the five topmost leaves on the stem that had not yet reached senescence at the time of harvesting. The chaff was analysed in samples from the 2020 harvest, except for finger millet which did not produce any panicles and hence chaff either in 2019 or 2020, and for those varieties of both sorghum and pearl millet that did not produce any panicles. The separation of plant parts, into top five or bulk leaves, and the addition of chaff for the analysis of the 2020 harvest were done to obtain data at a higher anatomical resolution than before. This decision was made after observing that, for the 2019 plants, the ratio of sensitive to fixed morphotypes from bulk leaves did not correlate with the type of watering. The model that we propose in this study is therefore based on phytoliths from different parts of the plant while the model published in D'Agostini et al. (2023) used only leaf phytoliths. Therefore, the dataset in this study improves our understanding of phytolith production in relation to water availability, and it has allowed us to build a more detailed and inclusive predictive model.

The phytoliths were analysed from a selected number of landraces and replicates to achieve statistical significance while minimising extraction and analytical time. Landraces that showed high diversity in both biomass production and transpiration efficiency were chosen to maximise the variations between the landraces and species. The same landraces were grown in the 2019 and 2020 seasons. In the 2019 crop we analysed two replicates from different cylinders for each

Table 1 Samples processed for phytolith extraction and final number of samples included in the analysis for each growing year

	2019			2020		
	WW	WS	*n*	WW	WS	*n*
Sorghum	12 bulk leaves	10 bulk leaves	22	21 top 5 leaves 21 bulk leaves 17 chaff	20 top 5 leaves 20 bulk leaves 14 chaff	113
Pearl millet	12 bulk leaves	10 bulk leaves	22	20 top 5 leaves 20 bulk leaves 20 chaff	20 top 5 leaves 20 bulk leaves 15 chaff	115
Finger millet	10 bulk leaves	8 bulk leaves	18	18 top 5 leaves 18 bulk leaves	18 top 5 leaves 17 bulk leaves	71
Total			62			311

of the two water treatments for four landraces of finger millet and five landraces each of pearl millet and sorghum. In addition, for two different genotypes of each species, both plants grown in the same WW cylinder were analysed to test any possible variability between replicates (D'Agostini et al. 2023). Given the variability found in the samples from 2019, the number of samples was increased for the 2020 samples. From these, we sampled three replicates from different cylinders for each of the two water treatments for four landraces of finger millet and five landraces each of pearl millet and sorghum. Two genotypes per species, both plants grown in the same cylinders for the two treatments, were analysed to test any possible variability between replicates. Microscopic examination of the 2020 samples showed that some included phytoliths from unrelated taxa indicating possible contamination, so to ensure accuracy, these samples were excluded from the analysis; the total number of samples included in the analysis is given in Table 1. Details about the phytolith samples as well as the analysed landraces with physiological data are given in the supporting data (ESM S2).

The method used for extracting phytoliths from the plant material combined dry ashing and wet oxidation techniques (D'Agostini et al. 2022a). An average of 604 phytoliths was counted for each slide (ESM S2) to reach the minimum number required for statistical representativeness of richness and evenness, which is typically set between 200 and 300 phytoliths (Strömberg 2009; Zurro 2018). Classification of morphotypes follows the available literature, especially Barboni and Bremond (2009), (Mercader et al. 2010); Gu et al. (2016). Nomenclature is based on the International Code for Phytolith Nomenclature (ICPN) 2.0, International Committee for Phytolith Taxonomy (ICPT 2019). The main morphotypes are listed in Table 2 and shown in Figs. 1 and 2. In this paper, we have chosen to refer to phytoliths using small capitals as in ICPN 2.0, but we do not use capitals for the cells in which the phytoliths formed (for example, bulliform cells). This implies that even generic categories of phytoliths, such as Bulliform or Elongate, are written in small capitals, covering broader classifications that are not connected to a specific morphotype defined by the code.

Table 2 Morphotypes identified from *Sorghum bicolor* (sorghum), *Cenchrus americanus* (pearl millet) and *Eleusine coracana* (finger millet)

Phytolith name following ICPN 2.0 (2019)	Corresponding images in Figs. 1 and 2
Acute bulbosus	a, b, u
Bilobate	c
Blocky	d, e
Bulliform flabellate	f
Cross	c
Elongate sinuate clavate	g
Elongate sinuate crenate	h
Elongate dentate	i
Elongate entire	j
Elongate sinuate	k, t
Polylobate	l
Rondel	m
Saddle	n, o, p
Stoma	q
Tracheary	r

Phytolith concentration was calculated for each identified morphotype and for the total phytoliths per sample using the same formula, below. The ratio of sensitive to fixed morphotypes has been estimated following the formula proposed by Jenkins et al. (2020). The equations used in this work are:

$$\text{Total phytoliths extracted} = \frac{(\text{total silica extracted (g)} \times \text{total phytoliths per slide})}{\text{total silica mounted (g)}}$$

$$\text{Concentration (in millions per gram of dry weight)} = \frac{\left(\frac{\text{total phytoliths extracted}}{\text{dry plant weight (g)}}\right)}{1{,}000{,}000}$$

$$\text{Sensitive/fixed ratio} = \frac{(\text{Elongate} + \text{Stoma})}{(\text{Cross} + \text{Bilobate} + \text{Polylobate} + \text{Rondel} + \text{Saddle})}$$

Statistical analysis

Total phytolith concentrations and ratios of sensitive to fixed morphotypes were normalised using the natural logarithm ($\log(x+1)$) to reduce skewness (Legendre and Legendre 2012). The relationship between these normalised variables and transpiration was tested using ANOVA.

Gaussian Generalised Linear Models (GLMs) were used to evaluate which explanatory variable (taxon, treatment or plant part) can better predict concentrations of individual morphotypes. GLMs were used instead of ANOVA since morphotype concentrations could not be normalised using standard transformations such as $\log(x+1)$ or square root. The p-value (set as 0.05 for significance) and the Akaike information criterion (AIC) were used to assess the significance of each model and to identify the model which provided the best prediction of a morphotype (Burnham et al. 2011).

A binomial GLM with stepwise selection was applied to the complete phytolith dataset to identify the best explanatory variables for phytolith morphotype percentages and the ratios of sensitive to fixed morphotypes that can distinguish between watering treatments (Peduzzi et al. 1980). For this

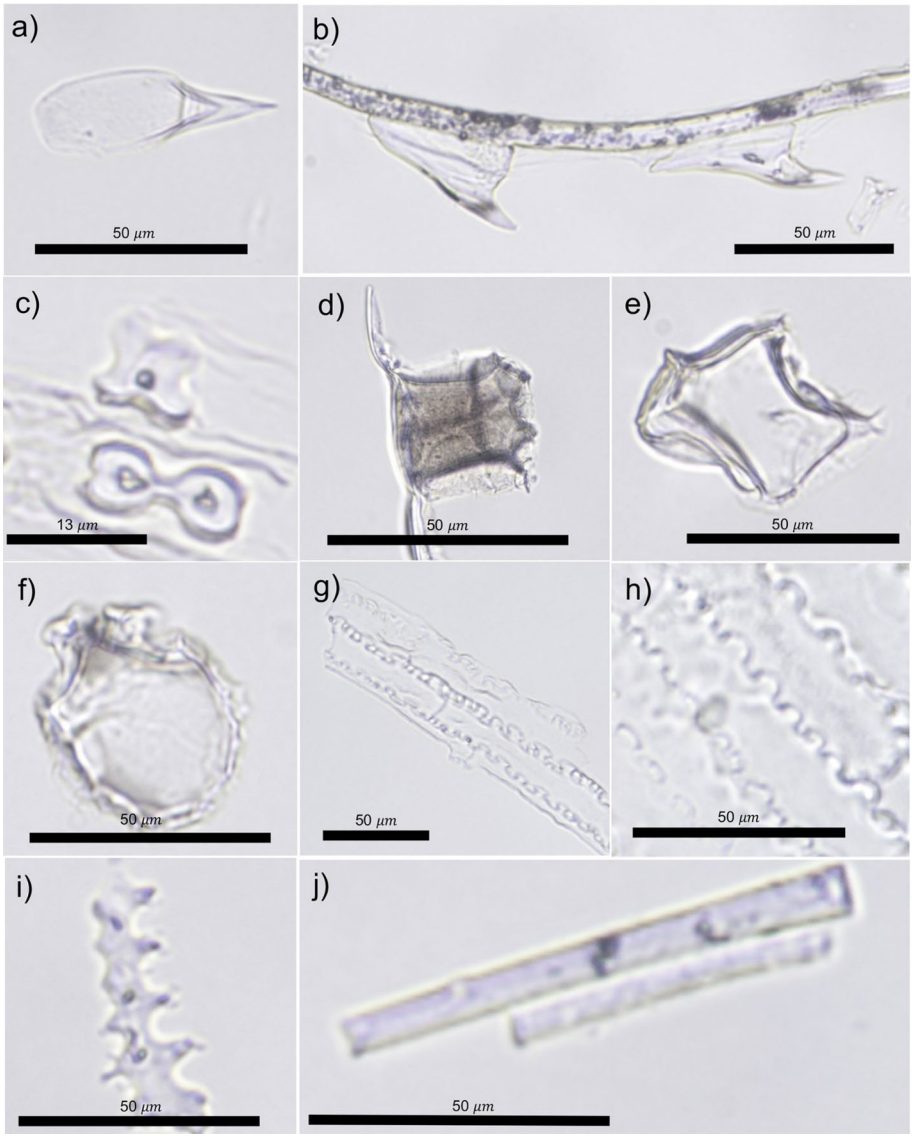

Fig. 1 Phytolith morphotypes extracted from the leaves and chaff. **a**, ACUTE BULBOSUS, *Eleusine* leaf, inner periclinal (IPS) view; **b**, silica skeleton of ACUTE BULBOSUS connected by an ELONGATE ENTIRE, *Cenchrus* leaf, side view; **c**, one BILOBATE and one CROSS in a silica skeleton, *Cenchrus* leaf, IPS view; **d**, silica skeleton with a BLOCKY, *Sorghum* leaf, side view; **e**, BLOCKY, *Eleusine* leaf, side view; **f**, BULLIFORM FLABELLATE, *Eleusine* leaf, side view; **g**, silica skeleton of ELONGATE SINUATE clavate, *Cenchrus* leaf, IPS view; **h**, silica skeleton of ELONGATE SINUATE crenate, *Sorghum* leaf. IPS view; **i**, ELONGATE DENTATE, *Sorghum* leaf. IPS view; **j**, silica skeleton of two ELONGATE ENTIRE, *Cenchrus* leaf, IPS view. This figure includes images that were previously published in D'Agostini et al. (2023) so to offer a direct comparison between the two years' harvests

analysis, morphotype concentrations were transformed to percentages so as to be comparable with phytolith data from soils or sediments, or samples different from modern plant parts. Logistic regression was then applied to predict the watering treatments (categorical output WW or WS), using morphotype percentages selected by the stepwise selection (Bruce et al. 2020).

Statistical analyses were done in R v. 4.3.1 using the packages ggplot2 v. 3.4.3, ggpubr v. 0.6.0, MASS v. 7.3–60 and tidyverse v. 2.0.0. Scripts are available in ESM S3.

Results

This research is a follow-up project to that published in D'Agostini et al. (2023). In our initial study, the results of the experimental crop of 2019 were presented and applied to a previously examined archaeological dataset (Lancelotti 2018). In this present study, we first made a detailed analysis of the 2020 experiment, using the same analytical method proposed in D'Agostini et al. (2023) for the samples of 2019. We then compared the results of the two experimental seasons, demonstrating consistency in phytolith production in the replicates. Finally, we suggest a model to predict water availability from the phytolith assemblage, incorporating both the 2019 and 2020 results into the analysis. This improves on the model from the preceding study with additional experimental data for enhanced detail and predictive accuracy.

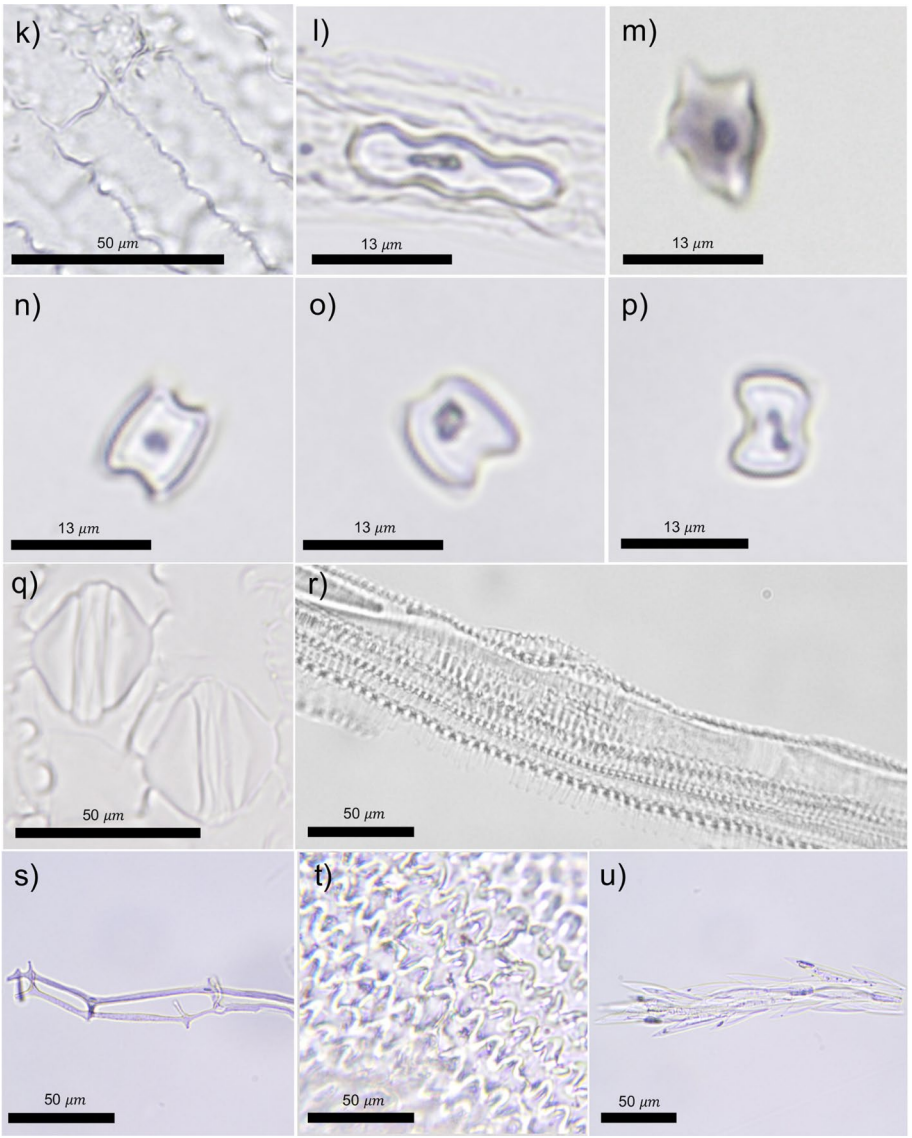

Fig. 2 Phytolith morphotypes continued. **k**, silica skeletons of ELONGATE SINUATE, *Cenchrus* leaf, inner periclinal (IPS) view; **l**, POLYLOBATE in a silica skeleton, *Cenchrus* leaf, IPS view; **m**, RONDEL with two spikes, apex of *Cenchrus* leaf, lateral view; **n**, SADDLE (short form), *Eleusine* leaf, side view; **o**, SADDLE (collapsed form), *Eleusine* leaf. side view; **p**, SADDLE (bilobed form), *Eleusine* leaf, IPS view; **q**, two STOMA in a silica skeleton, *Sorghum* leaf. IPS view; **r**, TRACHEARY structures, *Eleusine* leaf, IPS view; **s**, silicon structure identified as infilling (no phytoliths), *Cenchrus* leaves; **t**, silica skeletons of ELONGATE SINUATE, *Sorghum* chaff, IPS view; **u**, silica skeleton of ACUTE BULBOSUS connected by an ELONGATE ENTIRE, *Cenchrus* chaff, side view. This figure includes images that were previously published in D'Agostini et al. (2023), to offer a direct comparison between the two extractions

Phytolith production

Phytolith assemblages from the 2020 crop

When the three crops are analysed together, their phytolith concentrations show a moderately positive correlation with total water transpired, but only in samples from the top five leaves (Fig. 3). In both the bulk and top five leaf samples, all morphotypes showed higher concentrations in WW than in WS conditions. In chaff samples, BULLIFORM (sum of BLOCKY and BULLIFORM FLABELLATE), CROSS, ELONGATE SINUATE (excluding ELONGATE SINUATE clavate and ELONGATE SINUATE CRENATE), POLYLOBATE and STOMA showed higher concentrations in WS. However, bulliforms and stomata were scarcely present in the chaff. Complete data of each morphotype concentration, considering the three species together and separately, are given in ESM S2.

Considering the three species individually, the bulk leaves of *Sorghum bicolor* had a higher concentration of ACUTE BULBOSUS, CROSS, ELONGATE SINUATE clavate, ELONGATE ENTIRE and STOMA in WS conditions than in WW. The samples from the top five leaves of *Eleusine coracana* had a higher concentration of ELONGATE SINUATE clavate, ELONGATE DENTATE and RONDEL in WS. Leaves and chaff of *Cenchrus americanus* and *Eleusine coracana* always had higher total phytolith concentrations of all morphotypes together in WW than in WS plants (Fig. 4a). Complete data of each morphotype concentration, considering the three species together and separately, are given in ESM S2.

The total concentration of phytoliths and the proportion of sensitive to fixed morphotypes are not always correlated positively with the total water transpired (Figs. 4b and 5; Table 3). The sensitive to fixed ratio is not associated with the total water transpired, regardless of the taxon or the

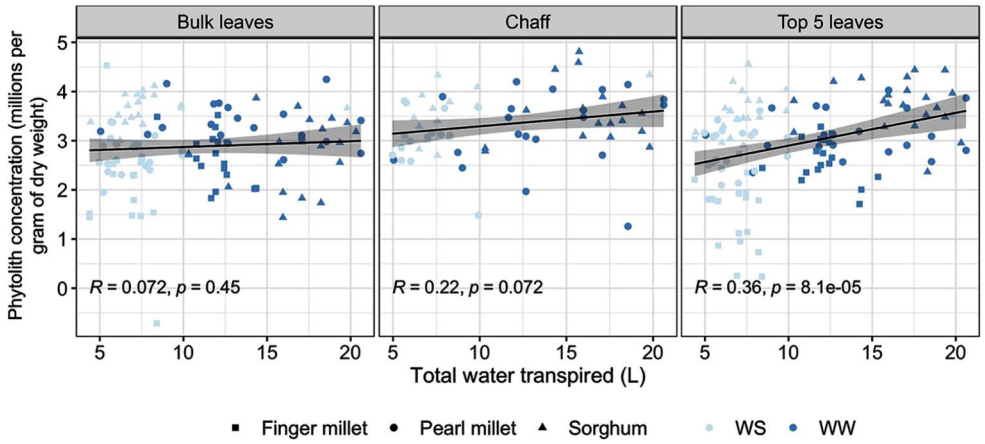

Fig. 3 Phytolith concentration as a function of total water transpired by particular plant parts. Grey bands represent 95% confidence intervals

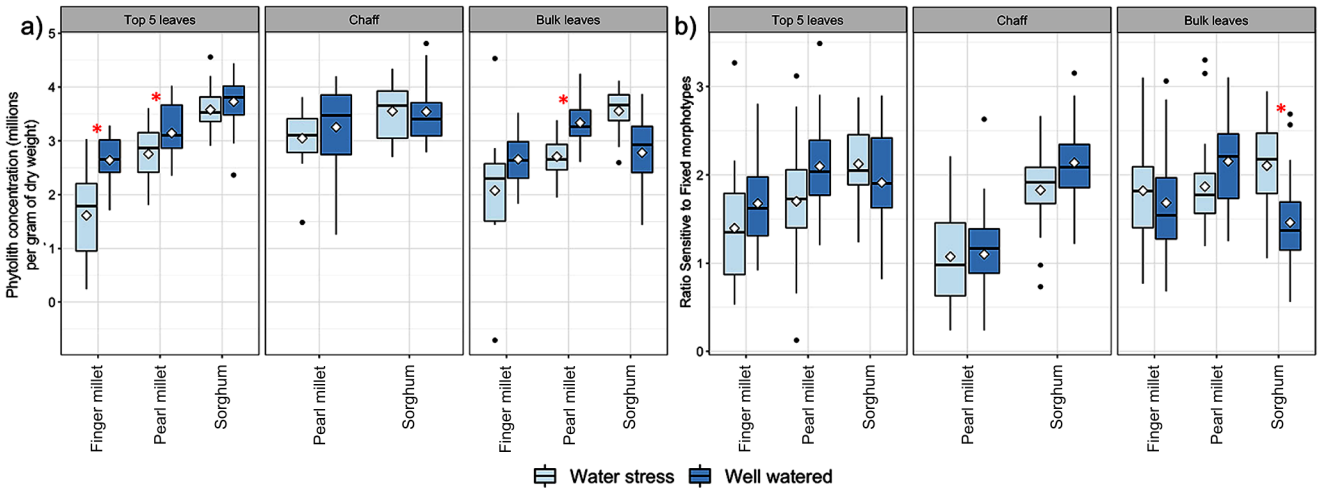

Fig. 4 Boxplot diagram showing **a**, phytolith concentrations; **b**, ratios of sensitive to fixed morphotypes in the 2020 harvest, grouped by crop and plant parts. Phytolith concentrations and ratios are normalised with natural logarithm (log(x + 1)). Red stars indicate significant differences between treatments. The precise p- and r-squared values are given in Table 3

Table 3 p- and r-squared values of the linear models tested, using total water transpired as an independent variable and phytolith concentration as a dependent variable for the plant parts of the three crops, top five leaves, bulk leaves and chaff. Statistically significant results with (p-values < 0.05 are marked with an asterisk (*)

		Top 5 leaves	Bulk leaves	Chaff
Sorghum	Phytolith concentration	p-value = 0.39 r = 0.14	p-value = 0.0014 * r = − 0.39	p-value = 0.4 r = 0.16
	Ratio of sensitive to fixed morphotypes	p-value = 0.055 r = -0.31	p-value = 0.024 * r = -0.36	p-value = 0.56 r = -0.11
Pearl millet	Phytolith concentration	p-value = 0.021 * r = 0.36	p-value = 0.009 * r = 0.41	p-value = 0.27 r = 0.19
	Ratio of sensitive to fixed morphotypes	p-value = 0.48 r = 0.12	p-value = 0.94 r = 0.012	p-value = 0.47 r = -0.13
Finger millet	Phytolith concentration	p-value = 0.014 * r = 0.41	p-value = 0.43 r = 0.14	NA
	Ratio of sensitive to fixed morphotypes	p-value = 0.22 r = 0.21	p-value = 0.29 r = -0.19	NA

specific part of the plant. Detailed analyses through linear regression and boxplots are given in ESM Figs. S2-S4.

Gaussian Generalised Linear Models (GLMs) indicate that the concentration of sensitive morphotypes is predicted by the water treatment, as for the morphotypes ACUTE BULBOSUS, BLOCKY, BULLIFORM FLABELLATE, the general category of BULLIFORM as the sum of all types of bulliform cell phytoliths, ELONGATE ENTIRE, ELONGATE SINUATE and

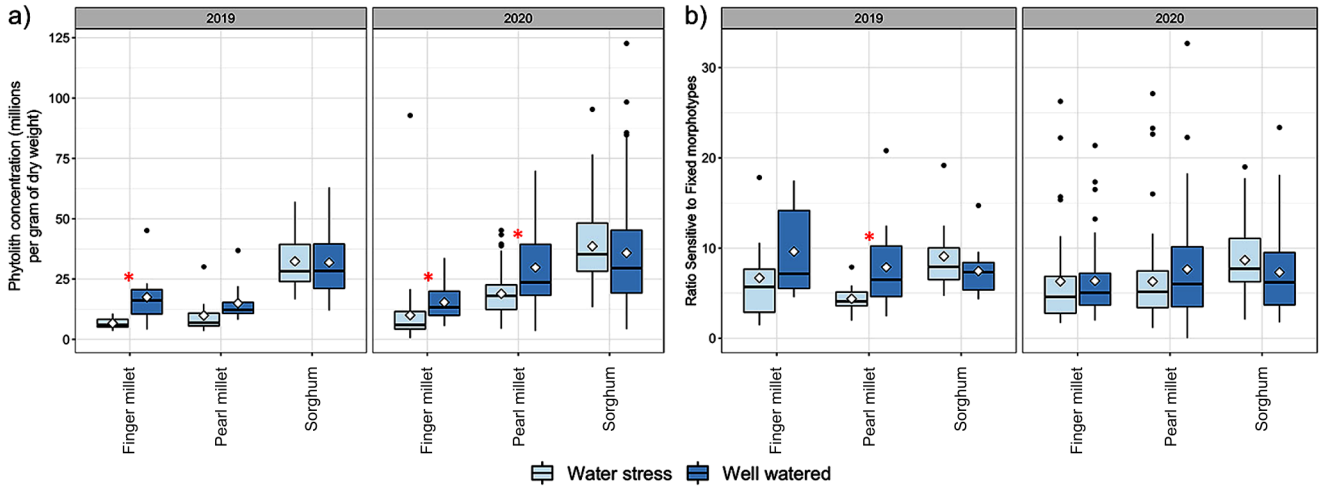

Fig. 5 Boxplot diagram showing **a**, phytolith concentration in millions per gram of dry weight; **b**, ratio of sensitive to fixed morphotypes in the crops of 2019 and 2020. Phytolith concentrations and ratios are normalised with natural logarithm (log(x + 1). Red stars indicate significant differences between treatments with p-values < 0.05

the general category of ELONGATE as the sum of all types of elongate cell phytoliths (Table 4). However, some taxa and plant parts are also good predictors of sensitive morphotype concentration, showing that their quantity does not depend exclusively on watering. Chaff has a good predictive capability, while sorghum can predict morphotype concentration.

Comparing the two experimental crops

E. coracana plants from both growing seasons showed differences in phytolith concentration between WW and WS treatments, with WW plants always accumulating more phytoliths (Fig. 5a). In instances where the variance in transpiration rates between WW and WS was minimal, there was a corresponding reduction in phytolith concentrations in the well watered plants (Fig. 5a; ESM Fig. S1). The same differences in *C. americanus* plants were only significant in the 2020 harvest. For *S. bicolor*, there were no significant differences in phytolith concentration between WW and WS, either from 2019 to 2020 (Fig. 5a; ESM Fig. S1). The ratio of sensitive to fixed morphotypes was significant only for pearl millet and only in the 2019 harvest, demonstrating that this ratio is not significant in showing differences in phytolith production with varying water availability for these three species (Fig. 5b).

Predictive model for water availability

The stepwise model used to test morphotype predictability when water treatments were used as dependent variables included data from the two growing seasons (2019 and 2020), the three species (*E. coracana*, *C. americanus* and *S. bicolor*) and all plant parts analysed (top five leaves, bulk leaves and chaff). Table 5 shows the results of the model where the best explanatory variables identified by the model have been used as predictors of the two water treatments; stepwise AIC (Akaike information criterion) 473.92, residual deviance 451.92, versus full model AIC 481.72, residual deviance 445.72. Among the morphotypes selected in this model, short cells show the best fit overall. Figure 6 shows the sigmoid predictions derived from the logistic regressions on the morphotypes that are predictive of water availability after the stepwise selection. Nevertheless, given that morphotype production differs between the three species and the water treatments, we decided to also explore the trend of logistic regressions in the three species separately (Table 5). A positive trend indicates that an increase in the percentage of a morphotype corresponds to a higher likelihood that the plant was grown under WW conditions; a negative trend suggests the contrary (ESM Figs S5-S16). The predictive responses of the morphotypes can be different for the three species and only BULLIFORM (sum of all types of bulliform cell phytoliths), ELONGATE ENTIRE and ELONGATE SINUATE are positively correlated to WW in the three species, while ELONGATE SINUATE clavate is negatively correlated.

Summary

As a summary, the results of the analysis presented here indicate that *Eleusine coracana* and *Cenchrus americanus* showed a positive relationship between transpiration rate and phytolith concentration from both experimental years (Figs. 4 and 5; ESM S3, S4; Table 3). The overall rate of phytolith production varied in WW plants as the transpiration process fluctuated in the two experimental growings

Table 4 P-values and Akaike information criteria (AIC) of the generalised linear models (GLM) tested using the two water treatments (WW, WS) and plant parts (top five leaves, bulk leaves and chaff) as independent variables. Since GLM uses n-1 interactions, treatment WS, species FM and plant part top five leaves are the first level factor on which comparisons are made, and thus they are not shown in the result score. Statistically significant results < 0.05 are shown by an asterisk (*), the higher the number, the greater the significance; three indicate with confidence that there are significant differences between the analysed variables for the concentration of a specific morphotype. Results at 0.08 > p-value > 0.05 that are almost statistically significant are shown with a dot (•). S, *Sorghum bicolor* (sorghum); PM, *Cenchrus americanus* (pearl millet

Morphotypes	Treatment (WW, WS)		Species (PM, S)		Plant part (chaff, bulk leaves)	
Sensitive Forms						
Acute bulbosus	WW p-value	0.0112*	PM p-value	1.74e-07***	Chaff p-value	5.71e-13***
	AIC	1871.2	S p-value	0.000712***	Bulk leaves p-value	0.0336*
			AIC	3495.2	AIC	1793.6
Bulliform (Blocky + B. flabellate)	WW p-value	0.00165**	PM p-value	0.2293	Chaff p-value	1.67e-05***
	AIC	-346.14	S p-value	0.0301*	Bulk leaves p-value	0.117
			AIC	-348.75	AIC	-353.16
Blocky	WW p-value	0.009768**	PM p-value	0.386497	Chaff p-value	8.16e-05***
	AIC	-384.11	S p-value	0.020384*	Bulk leaves p-value	0.123
			AIC	-388.83	AIC	-391.18
Bulliform flabellate	WW p-value	0.000269***	PM p-value	0.0497*	Chaff p-value	0.00297**
	AIC	-1538.5	S p-value	0.8934	Bulk leaves p-value	0.59698
			AIC	-1528.8	AIC	-1533
Elongate (all Elongates)	WW p-value	0.0301*	PM p-value	0.00372**	Chaff p-value	0.119
	AIC	3087.1	S p-value	< 2e-16	Bulk leaves p-value	0.403
			AIC	2998.8	AIC	3088.3
Elongate sinuate clavate	WW p-value	0.603	PM p-value	0.00324**	Chaff p-value	0.000769***
	AIC	2860	S p-value	< 2e-16***	Bulk leaves p-value	0.051733*
			AIC	2744.1	AIC	2850.7
Elongate sinuatecrenate	WW p-value	0.1549	PM p-value	0.158902	Chaff p-value	0.908486
	AIC	-517.19	S p-value	0.123684	Bulk leaves p-value	0.000891***
			AIC	-515.91	AIC	-527.8
Elongate dentate	WW p-value	0.110	PM p-value	0.7888	Chaff p-value	2.13e-07***
	AIC	1820	S p-value	0.0212*	Bulk leaves p-value	0.685
			AIC	1814.9	AIC	1792.3
Elongate entire	WW p-value	2.03e-06***	PM p-value	0.77490	Chaff p-value	8.01e-08***
	AIC	1897.8	S p-value	0.00293**	Bulk leaves p-value	0.415
			AIC	1910	AIC	1889.8
Elongate sinuate	WW p-value	0.00138**	PM p-value	0.0377*	Chaff p-value	4.8e-07***
	AIC	2453.7	S p-value	1.06e-06***	Bulk leaves p-value	0.427
			AIC	2440.7	AIC	2437.4
Stoma	WW p-value	0.287	PM p-value	0.687	Chaff p-value	1.51e-07***
	AIC	808.99	S p-value	4.71e-11***	Bulk leaves p-value	0.042*
			AIC	749.65	AIC	784.04
Fixed forms						
Bilobate	WW p-value	0.28689	PM p-value	0.0761 •	Chaff p-value	0.75326
	AIC	1855.2	S p-value	3.69e-05***	Bulk leaves p-value	0.60055
			AIC	1840.3	AIC	1857.7
Cross	WW p-value	0.576	PM p-value	1.11e-11***	Chaff p-value	2.41e-09***
	AIC	1773.9	S p-value	2.44e-15***	Bulk leaves p-value	0.176
			AIC	1707.5	AIC	1720.1
Polylobate	WW p-value	0.3218	PM p-value	0.1019	Chaff p-value	0.721
	AIC	585.87	S p-value	0.0477*	Bulk leaves p-value	0.218
			AIC	584.59	AIC	586.21
Rondel	WW p-value	0.097207 •	PM p-value	1.07e-06***	Chaff p-value	0.440579
	AIC	-104.77	S p-value	3.97e-07***	Bulk leaves p-value	0.095756 •
			AIC	-130.93	AIC	-105.87
Saddle	WW p-value	0.0369*	PM p-value	< 2e-16***	Chaff p-value	0.00283**
	AIC	966.88	S p-value	< 2e-16***	Bulk leaves p-value	0.99126
			AIC	701.71	AIC	961.76

Table 5 Results of the stepwise selection and logistic regression to predict water treatment from morphotype percentage. The model used phytolith morphotype percentage and the ratio of sensitive to fixed morphotype as predictors and treatment (WW, WS) as dependent variables. The third column describes the correlation of the sigmoidal curves observed in the logistic regressions conducted on the predictive morphotypes against the WW treatment for the three species separately. Statistically significant results at p-value < 0.05 are marked with an asterisk (*), the greater the number, the higher the certainty of the significance of the results; three asterisks indicates with confidence that the morphotype percentage is a good explanatory variable to differentiate WW and WS. Statistically almost significant results at 0.08 > p-value > 0.05 are marked with a dot (•)

	Stepwise model *p*-value	Correlation between WW condition and morphotype
Ratio sensitive to fixed morphotypes	0.20172 (excluded by stepwise selection)	
Sensitive forms		
Acute bulbosus	0.015059*	Finger millet: negative Pearl millet: positive Sorghum: negative
Bulliform (Blocky + B. flabellate)	0.069513•	Finger millet: positive Pearl millet: positive Sorghum: positive
Blocky	0.37185 (excluded by stepwise selection)	
Bulliform flabellate	0.37185 (excluded by stepwise selection)	
Elongate (all Elongates)	0.97998 (excluded by stepwise selection)	
Elongate sinuateclavate	0.000237***	Finger millet: negative Pearl millet: negative Sorghum: negative
Elongate sinuatecrenate	0.97972 (excluded by stepwise selection)	
Elongate dentate	0.002461**	Finger millet: negative Pearl millet: positive Sorghum: positive
Elongate entire	0.005109**	Finger millet: positive Pearl millet: positive Sorghum: positive
Elongate sinuate	0.001761**	Finger millet: positive Pearl millet: positive Sorghum: positive
Stoma	0.23123 (excluded by stepwise selection)	
Fixed forms		
Bilobate	0.14493 (excluded by stepwise selection)	
Cross	0.000149***	Finger millet: positive Pearl millet: negative Sorghum: positive
Polylobate	0.019280*	Finger millet: positive Pearl millet: negative Sorghum: positive
Rondel	0.000476***	Finger millet: negative Pearl millet: positive Sorghum: positive
Saddle	0.000349***	Finger millet: negative Pearl millet: positive Sorghum: positive

whereas it remained constant in WS ones, as did the transpiration rate (Fig. 2; ESM S1). *Sorghum bicolor*, on the contrary, not only tends to accumulate more phytoliths in general (Figs. 4 and 5), but additionally, the variation between the phytolith production of WW and WS plants significantly depends on the specific plant part concerned (Fig. 4; ESM S2). When we examine the production of specific morphotypes, finger millet tends to increase its production of Elongate sinuate clavate, Elongate dentate and Rondel under WS conditions only in the samples from the top five leaves, but *C. americanus* yields more Bulliform, Stoma, and Polylobate morphotypes in chaff (even more so than *S. bicolor*), and *S. bicolor*, under water stress conditions, produces more Acute bulbosus, Cross, Elongate sinuate clavate, Elongate entire and Stoma morphotypes both in the leaves and chaff (Table 5; ESM S2, S5-S12).

The calculated ratio of sensitive to fixed morphotypes is consistently unrelated to watering (Figs. 4 and 5; Tables 3 and 5). Nonetheless, some morphotypes have proved to be highly predictive, both sensitive (Acute bulbosus, Bulliform, Elongate sinuate Elongate sinuate clavate, Elongate dentate and Elongate entire) and fixed (Cross,

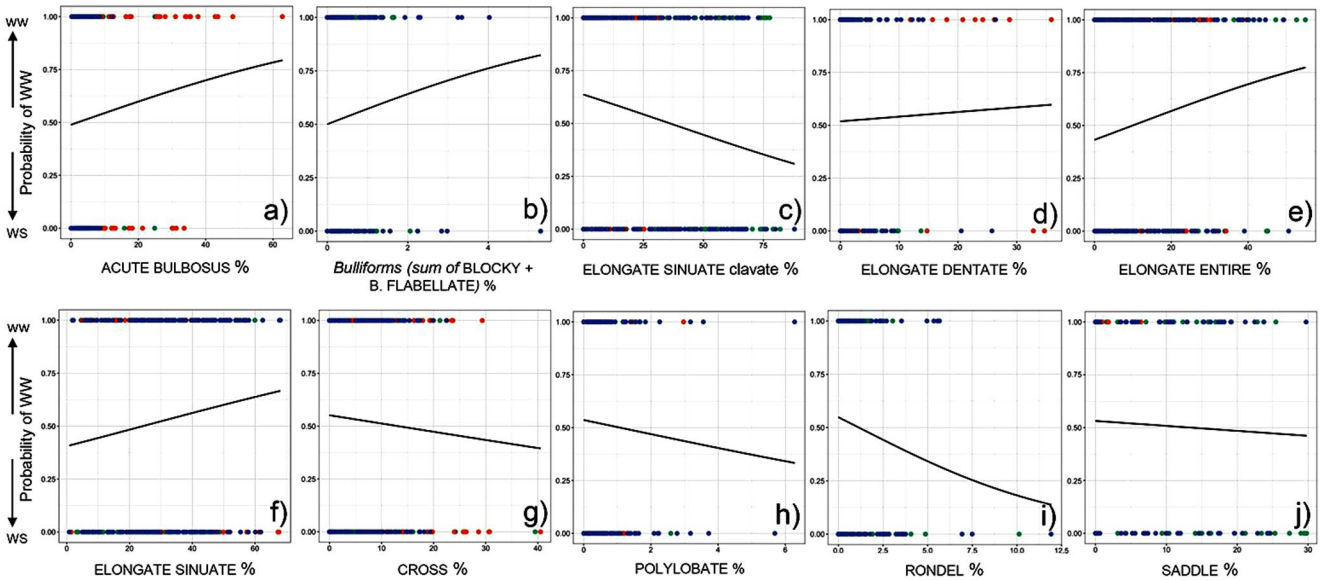

Fig. 6 Logistic regression plots of the morphotypes predictive of water availability considering the three crops together (Table 4). **a**, Acute bulbosus; **b**, Bulliform; **c**, Elongate sinuate clavate; **d**, Elongate dentate; **e**, Elongate entire; **f**, Elongate sinuate; **g**, Cross; **h**, Polylobate; **i**, Rondel; **j**, Saddle. Percentages of each morphotype shown on X axis. The colours of the dots correspond to the plant parts analysed; bulk leaves, blue; top five leaves, green; chaff samples, orange

Polylobate, Rondel and Saddle), and the only ones that are been consistently predictive in all three species are Bulliform, Elongate entire, Elongate sinuate and Elongate sinuate clavate (Table 5).

Discussion

In our analysis of C_4 millet and sorghum landraces from arid areas of East Africa and South Asia, we demonstrate that short cell phytoliths (fixed morphotypes), Elongate and Bulliform (sensitive morphotypes), as well as Acute bulbosus, traditionally omitted from the ratio of sensitive to fixed morphotypes according to Madella et al. (2009) and Jenkins et al. (2016), are all predictive morphotypes for plant water availability. Among specific morphotypes, Elongate sinuate clavate, Cross, Rondel and Saddle proved to be the most reliable predictors (Table 4). Within the highly predictive morphotypes, a consistent predictive pattern emerged, with either positive or negative correlations between Bulliform, Elongate entire, Elongate sinuate and Elongate sinuate clavate with water availability in all three species. On the basis of such results, we propose a model that uses logistic regression, which allows the probability of a discrete variable (WW or WS) to be modelled using independent variables such as the percentages of morphotypes.

An advantageous aspect of this research is that the predictions from the model presented in this study can be applied to various phytolith assemblages. The generic morphotypes that are present in several plant groups, such as Bulliform or Elongate entire, can be used as predictors of water availability when investigating ancient assemblages produced by a mix of different plants of unknown origins. Otherwise, morphotypes that are characteristic of a specific group of plants (family, genus or species), namely Acute bulbosus, Elongate sinuate, Elongate sinuate clavate, Cross, Rondel and Saddle, can be used to predict water availability in assemblages mainly formed by those plants. For example, the full model as presented here can be applied to archaeological contexts where *E. coracana*, *C. americanus* and *S. bicolor* are considered to be the main taxa contributing to the assemblage because they have been identified through alternative means, such as charred grains or also where the presence of other crops is considered negligible, as in the arid regions of South Asia and the Horn of Africa, which are the geographical origins of the landraces examined in this study. The proposed model can be used to formulate hypotheses about crop management in agricultural settings where other direct proxies for irrigation are limited or cannot be found. As demonstrated by D'Agostini et al. (2023), the model was successfully applied to published data from the Mature Harappan (Indus Valley Civilisation) period contexts in northwest South Asia with differing environmental conditions (Lancelotti 2018). Furthermore, both the model and the basic phytolith dataset can function as validation data. For example, in the study by Ruiz-Giralt et al. (2023a) the model was used to validate the findings of the ethnographic/climatic modelling.

One of the advantages of using a predictive model based on a wide range of morphotypes produced by cells from various plant parts in different species simultaneously is that it can be applied to archaeological contexts independently of their geographical location or chronology, as long as the criteria listed above are respected. In our previous publication (D'Agostini et al. 2023) the prediction model relied solely on the assemblage of phytoliths produced by bulk leaves, while the current study also incorporates the top five leaves and chaff. As a consequence, certain details of the model have undergone changes, demonstrating how the inclusion of various plant parts from several taxa in the analysis has contributed to refining the model. For example, in addition to Polylobate, the model now includes also Acute bulbosus, Elongate sinuate, Elongate entire and Elongate dentate, as well as various short cells such as Cross, Rondel and Saddle as good water predictors. Meanwhile, the predictive power of Stoma and Blocky (typically found only in leaves) has decreased (Table 5). This model provides an innovative methodological tool for the archaeological investigation of early farming practices in dry lands. Indeed, the construction of a modern starting point for applying logistic regressions to predict the availability of water from phytolith assemblages from various taxa can be extended to different ecological regions, provided that our model is based on plants likely to be found in dry land agricultural contexts. By expanding the modern basic data with a broader range of taxa from diverse environmental settings it would be possible to extend the future archaeological applicability of the model.

However, the results obtained, when viewed from the perspective of plant science, warrant a more detailed discussion. They demonstrate a complex relationship between C_4 phytolith accumulation and transpiration in the three studied species, revealing that:

a. The three C_4 species show a great variability between them in the amounts of phytolith morphotypes produced in different plant parts under particular regimes of water supply (Tables 4 and 5). This suggests that the plants, while all regulating their biosilica deposition in response to watering, do so in different ways, prompting us to reconsider how we interpret archaeological assemblages from phytolith data that treat all plants as equivalents. This also brings into question the usefulness of the established ratio between sensitive and fixed morphotypes, which will be discussed below.
b. Contrary to the prevailing assumption suggesting that increased water availability corresponds to a rise in biomass and consequently also in phytolith production, or a relative increase in sensitive morphotypes (for example, Sangster et al. 2001; Jenkins et al. 2020), this study shows that predictive morphotypes are not necessarily more abundant from WW conditions and actually such significant morphotypes can be produced more abundantly under WS conditions (Table 5). This increased production is relevant for understanding the role of phytoliths as a response mechanism to abiotic stresses such as drought.

The findings from our work are consistent with previous studies on the role of silica in plant systems, despite the existence of some controversial aspects that remain to be studied, such as whether there is a direct connection between transpired water and biosilica precipitation. Hosseini et al. (2017) suggested that silicon could play a fundamental role in the response of plants to water stress conditions by delaying osmotic leaf senescence (leaf ageing induced by osmotic stress that disrupts the water balance). This happens by increasing chlorophyll levels and by regulating abscisic acid plant hormone which helps the stomata to close and inhibits growth, and which increases under drought conditions. Opaline silica could also form a thin layer in epidermal tissues that may increase the rigidity of delicate plant parts and prevent water loss (Yoshida et al. 1962; Rodrigues et al. 2003). In our study, the morphotypes showing higher concentrations under conditions of water stress (Acute Bulbosus, Cross, Elongate and Stoma) have previously been shown to play a role in improving drought resistance. Silicification of stomata seems to help in reducing transpiration by regulating water loss (Goto et al. 2003; Hosseini et al. 2017; Gao et al. 2020). Cross morphotypes may form preferentially on the sides of minor leaf veins of sorghum, allowing flow through the xylem to continue (Kaufman et al. 1985; Kumar et al. 2017). Elongate, from the epithelial cells of both leaves and chaff, would increase light absorption by altering the photochemistry (Cooke and Leishman 2016) and hardening the tissues, particularly fragile under WS conditions, which can prevent pathogen attack or grazing and crumpling of the leaf blade (Yoshida et al. 1962; Rodrigues et al. 2003; Meunier et al. 2017). Silicified trichomes, which have been proven to respond to attack by pathogens (Fauteux et al. 2005; Mateos-Naranjo et al. 2013; Daoud et al. 2018; Oliva et al. 2021), have also been found to be more abundant in dry environments (Olsen et al. 2013). Therefore, our data further support the hypothesis that the production of particular morphotypes could be linked to the physiological needs of the plant.

c. We need to redefine the categories used to calculate the ratio between sensitive and fixed morphotypes (for example, Madella et al. 2009 and Jenkins et al. 2020) and this study may mark the beginning of a new discussion on the topic. In our study, the ratio of sensitive to fixed morphotypes is

poorly correlated to total water transpired, most probably due to differences in the deposition of phytoliths between various taxa. The ratio published in the literature includes STOMA among the sensitive morphotypes, but it does not include BULLIFORM or ACUTE BULBOSUS (trichomes), which were found to be sensitive to watering in our study. Silicified stomata in a leaf that is still photosynthesising could lead to poor regulation of normal leaf development (Kumar et al. 2017) and thus we believe that STOMA should be included in the group of phytoliths whose deposition is most probably genetically regulated, at least for the timing of silicification, which cannot occur while the leaf is still developing (Motomura 2004). In contrast, bulliforms not only have a water storage function as living cells, but also the deposition of Si in these cells has been linked to rainfall, as BULLIFORM size increases in wet environmental conditions (Wang et al. 2019). Similarly, in some taxa the silicification of trichomes tends to be higher in dry environments with low soil moisture (Olsen et al. 2013). Therefore, we suggest that it would be more appropriate to classify phytoliths into morphotypes whose deposition is caused by the ability of the plant to react to water stress conditions, such as CROSS phytoliths that perform an active function in protecting the plant from the adverse effects of drought (for example, Kumar et al. 2017). Also, morphotypes directly formed by precipitation after loss of water by transpiration, such as BULLIFORM, whose formation as a morphotype has never been related to potential drought responses, although we know that both its functions in living cells and its formation mode as a phytolith are closely linked to transpiration (Grigore and Toma 2017). Both mechanisms of morphotype formation would depend either on the amount of water available for transpiration or on the way the plants are genetically enabled to respond to water stress.

Further methodological advances arise from the experimental methods used for this work, which are also relevant to the field of experimental archaeobotany. The use of lysimeters for controlled plant growth, allowing precise calculation of plant transpiration, enables the direct exploration of the relationship between phytolith formation and plant physiology by excluding the effects of unknown variables in the complex water cycle of interactions between the plants, soil and air (Katz et al. 2013; Jenkins et al. 2016).

Conclusions

In this study we have developed a prediction model for water availability to growing plants and specifically grasses, using the particular assemblages of phytoliths produced by the C_4 crops sorghum, finger millet and pearl millet. The model can be used to interpret past agricultural land and water management in dry regions from archaeological phytolith assemblages from sites where such C_4 crops were present (for example, D'Agostini et al. 2023; Ruiz-Giralt et al. 2023a). It could be a valuable tool for multi-proxy research and hypothesis formulation on the growing of crops where there are few other sources of evidence about irrigation. The reliability of the model rests on the response of phytolith production to water availability for transpiration, which is different at taxon and morphotype levels. The three studied species produce different arrays of morphotypes, but BULLIFORM, ELONGATE ENTIRE, ELONGATE SINUATE and ELONGATE SINUATE clavate were found to be significant in relation to water availability in all three and can therefore be used to assess water availability, regardless of the crop from which they came. Of these, BULLIFORM, ELONGATE ENTIRE and ELONGATE SINUATE are positively correlated to well watered conditions, while ELONGATE SINUATE clavate is negatively correlated. The outcomes derived from our predictive model agree with the findings from other plant studies, suggesting a connection between specific functions and the production of certain phytolith types (for example, Kumar et al. 2017). The application of our model to archaeological material would improve our understanding of past water management for farming in dry lands where C_4 crops have traditionally been grown. These are key areas for understanding the possibly resilient dynamics of crop growing, that might still have significance for devising policies for small-scale, non-industrialised farming at the present day, a current reality in many parts of the world.

Acknowledgements We would like to thank the GEMS team from ICRISAT who helped during the experimental work in the fields. We are also thankful to Jordi Ibañez Insa and Soledad Alvarez of the Geosciences Barcelona (GEO3BCN-CSIC) for conducting the XRF analysis of the sediments. This work is part of the RAINDROPS project funded by the European Research Council (ERC-Stg-2017) under grant agreement n. 759800. University Pompeu Fabra health and safety regulations have been followed during both the fieldwork and the laboratory work. RAINDROPS has received ethical approval from the Institutional Committee for Ethical Review of Projects (CIREP) at Universitat Pompeu Fabra (ethics certificate n. 2017/7662/I). VV was partially supported by the Make Our Planet Great Again (MOPGA) ICARUS project (Improve Crops in Arid Regions and future climates) funded by the Agence Nationale de la Recherche (ANR, grant ANR-17-MPGA-0011). CASEs (UPF) is a Quality Research Group recognised by Agencia de Gestión de Ayudas Universitarias y de Investigación (the Catalan Agency for Research) (AGAUR-SGR 212).

Author contributions Conceptualization: D'Agostini, Ruiz-Pérez, Lancelotti; Methodology: D'Agostini, Ruiz-Pérez, Vadez, Lancelotti; Formal analysis and investigation: D'Agostini; Writing-original draft preparation: D'Agostini; Writing review and editing: D'Agostini, Ruiz-Pérez, Madella, Vadez, Lancelotti; Funding acquisition: Madella, Lancelotti; Resources: Madella, Vadez, Lancelotti; Supervision: Madella, Vadez, Lancelotti.

Data availability Supporting data (ESM) are available on Zenodo at https://doi.org/10.5281/zenodo.10246367.

Declarations

Competing interests All authors certify that they have no direct or indirect affiliations with or involvement in any organisation or entity with any financial or non-financial interest in the subject matter or materials discussed in this manuscript. The authors have no financial or proprietary interests in any material discussed in this manuscript.

References

Araus JL, Febrero A, Buxó R et al (1997) Identification of Ancient Irrigation practices based on the Carbon Isotope discrimination of Plant seeds: a case study from the South-East Iberian Peninsula. J Archaeol Sci 24:729–740. https://doi.org/10.1006/jasc.1997.0154

Balbo AL, Gómez-Baggethun E, Salpeteur M et al (2016) Resilience of small-scale societies: a view from drylands. Ecol Soc 21:53. https://doi.org/10.5751/ES-08327-210253

Barboni D, Bremond L (2009) Phytoliths of east African grasses: an assessment of their environmental and taxonomic significance based on floristic data. Rev Palaeobot Palynol 158:29–41. https://doi.org/10.1016/j.revpalbo.2009.07.002

Beldados A, Ruiz-Giralt A (2023) Burning questions: experiments on the effects of charring on domestic and wild sorghum. J Archaeol Sci Rep 51:104170. https://doi.org/10.1016/j.jasrep.2023.104170

Biagetti S, Ruiz-Giralt A, Madella M et al (2021) No rain, no grain? Ethnoarchaeology of Sorghum and Millet Cultivation in Dryland environments of Sudan, Parkistan, and Ethiopia. Ethnoarchaeology 13:80–104. https://doi.org/10.1080/19442890.2022.2059994

Bremond L, Alexandre A, Peyron O, Guiot J (2005) Grass water stress estimated from phytoliths in West Africa. J Biogeogr 32:311–327. https://doi.org/10.1111/j.1365-2699.2004.01162.x

Bruce P, Bruce A, Gedeck P (2020) Practical statistics for data scientists: 50+essential concepts using R and Python, 2nd edn. O'Reilly Media, Sebastopol

Burnham KP, Anderson DR, Huyvaert KP (2011) AIC model selection and multimodel inference in behavioral ecology: some background, observations, and comparisons. Behav Ecol Sociobiol 65:23–35. https://doi.org/10.1007/s00265-010-1029-6

Climate North West Knowledge (2022) (Climate North West Knowledge 2022) https://climate.northwestknowledge.net, accessed on 22 August 2022)

Cooke J, Leishman MR (2016) Consistent alleviation of abiotic stress with silicon addition: a meta-analysis. Funct Ecol 30:1:340–1357. https://doi.org/10.1111/1365-2435.12713

Coskun D, Deshmukh R, Shivaraj SM et al (2021) Lsi2: a black box in plant silicon transport. Plant Soil 466. https://doi.org/10.1007/s11104-021-05061-1

Critchley W, Gowing J (eds) (2012) Water harvesting in Sub-saharan Africa. Routledge, New York

D'Agostini F, Ruiz-Pérez J, Madella M et al (2022a) Phytolith extraction and counting procedure for modern plant material rich in silica skeletons. protocols.io. https://doi.org/10.17504/protocols.io.q26g74mb8gwz/v2

D'Agostini F, Vadez V, Kholova J et al (2022b) Understanding the relationship between Water availability and Biosilica Accumulation in selected C_4 Crop leaves: an Experimental Approach. Plants 11:1019. https://doi.org/10.3390/plants11081019

D'Agostini F, Ruiz-Pérez J, Madella M et al (2023) Phytoliths as indicators of plant water availability: the case of millets cultivation in the Indus Valley civilization. Rev Palaeobot Palynol 309:104783. https://doi.org/10.1016/j.revpalbo.2022.104783

D'Andrea AC, Fahmy AG, Perry L et al (2015) Ancient agricultural economy in the Horn of Africa: new evidence from grinding stones and stable isotopes. 8th International Workshop for African Archaeobotany (IWAA), Modena and Reggio Emilia, 23–26 June 2015. Atti Soc Nat Mat Modena 46(Suppl):155–157

D'Odorico P, Bhattachan A (2012) Hydrologic variability in dryland regions: impacts on ecosystem dynamics and food security. Philos Trans R Soc B Biol Sci 367:3:145–3157. https://doi.org/10.1098/rstb.2012.0016

Daoud AM, Hemada MM, Saber N, El-Araby AA, Moussa L (2018) Effect of Silicon on the Tolerance of Wheat (*Triticum aestivum* L.) to salt stress at different growth stages: Case Study for the management of Irrigation Water. Plants 7:29. https://doi.org/10.3390/plants7020029

Ermish BJ, Boomgarden SA (2022) Identifying water availability with maize phytoliths in Range Creek Canyon, Utah. J Archaeol Sci Rep 41:103267. https://doi.org/10.1016/j.jasrep.2021.103267

Fauteux F, Rémus-Borel W, Menzies JG, Bélanger RR (2005) Silicon and plant disease resistance against pathogenic fungi. FEMS Microbiol Lett 249:1–6. https://doi.org/10.1016/j.femsle.2005.06.034

Ferrio JP, Araus JL, Buxó R, Voltas J, Bort J (2005) Water management practices and climate in ancient agriculture: inferences from the stable isotope composition of archaeobotanical remains. Veget Hist Archaeobot 14:510–517. https://doi.org/10.1007/s00334-005-0062-2

Gao C, Wang M, Ding L et al (2020) High water uptake ability was associated with root aerenchyma formation in rice: evidence from local ammonium supply under osmotic stress conditions. Plant Physiol Biochem 150:171–179. https://doi.org/10.1016/j.plaphy.2020.02.037

Goto M, Ehara H, Karita S et al (2003) Protective effect of silicon on phenolic biosynthesis and ultraviolet spectral stress in rice crop. Plant Sci 164:349–356. https://doi.org/10.1016/S0168-9452(02)00419-3

Grigore M-N, Toma C (2017) Bulliform cells. In: Grigore M-N, Toma C (eds) Anatomical adaptations of Halophytes: a review of Classic Literature and recent findings. Springer, Cham, pp 325–338

Gu Y, Liu H, Wang H, Li R, Yu J (2016) Phytoliths as a method of identification for three genera of woody bamboos (Bambusoideae) in tropical southwest China. J Archaeol Sci 68:46–53. https://doi.org/10.1016/j.jas.2015.08.003

Hodson MJ, White PJ, Mead A, Broadley MR (2005) Phylogenetic variation in the Silicon Composition of Plants. Ann Bot 96:1027–1046. https://doi.org/10.1093/aob/mci255

Hosseini SA, Maillard A, Hajirezaei MR et al (2017) Induction of Barley Silicon Transporter *HvLsi1* and *HvLsi2*, increased silicon concentration in the shoot and regulated starch and ABA Homeostasis under osmotic stress and concomitant Potassium Deficiency. Front Plant Sci 8:1359. https://doi.org/10.3389/fpls.2017.01359

International Institute for Environment and Development (2022) International Institute for Environment and Development (IIED), www.iied.org, accessed on 23 April 2022

International Committee for Phytolith Taxonomy (ICPT) (2019) International Code for Phytolith nomenclature (ICPN) 2.0. Ann Bot 124:189–199. https://doi.org/10.1093/aob/mcz064

Jenkins E (2009) Phytolith taphonomy: a comparison of dry ashing and acid extraction on the breakdown of conjoined phytoliths formed in *Triticum durum*. J Archaeol Sci 36:2:402–2407. https://doi.org/10.1016/j.jas.2009.06.028

Jenkins E, Jamjoum K, Nuimat S et al (2016) Identifying ancient water availability through phytolith analysis: an experimental approach.

J Archaeol Sci 73:82–93. https://doi.org/10.1016/j.jas.2016.07.006

Jenkins EL, Predanich L, Al Nuimat S et al (2020) Assessing past water availability using phytoliths from the C_4 plant *Sorghum bicolor*: an experimental approach. J Archaeol Sci Rep 33:102460. https://doi.org/10.1016/j.jasrep.2020.102460

Katz O (2019) Silicon content is a plant functional trait: implications in a changing world. Flora 254:88–94. https://doi.org/10.1016/j.flora.2018.08.007

Katz O, Gilead I, Bar (Kutiel) P, Shahack-Gross R (2007) Chalcolithic Agricultural Life at Grar, Northern Negev, Israel: Dry Farmed cereals and Dung-Fueled hearths. Paléorient 33:101–116. https://doi.org/10.3406/paleo.2007.5223

Katz O, Lev-Yadun S, Bar (Kutiel) P (2013) Plasticity and variability in the patterns of phytolith formation in Asteraceae species along a large rainfall gradient in Israel. Flora - Morphol Distrib Funct Ecol Plants 208:438–444. https://doi.org/10.1016/j.flora.2013.07.005

Kaufman PB, Dayanandan P, Franklin CI, Takeoka Y (1985) Structure and function of silica bodies in the epidermal system of Grass shoots. Ann Bot 55:487–507. https://doi.org/10.1093/oxfordjournals.aob.a086926

Kumar S, Soukup M, Elbaum R (2017) Silicification in Grasses: variation between different cell types. Front Plant Sci 8:438. https://doi.org/10.3389/fpls.2017.00438

Kumar EA, Kumar S, Mandapati J, Peachey R (2023) Innovations to transform drylands. International Crops Research Insitute for the Semi-Arid Tropics

Lancelotti C (2018) Not all that burns is wood'. A social perspective on fuel exploitation and use during the Indus urban period (2600 – 1900 BC). PLoS ONE 13:e0192364. https://doi.org/10.1371/journal.pone.0192364

Legendre P, Legendre L (2012) Numerical ecology, 3rd edn. Elsevier, Amsterdam

Lux A, Luxova M, Hattori T et al (2002) Silicification in sorghum (*Sorghum bicolor*) cultivars with different drought tolerance. Physiol Plant 115:87–92. https://doi.org/10.1034/j.1399-3054.2002.1150110.x

Ma JF, Yamaji N (2006) Silicon uptake and accumulation in higher plants. Trends Plant Sci 11:392–397. https://doi.org/10.1016/j.tplants.2006.06.007

Madella M, Lancelotti C (2012) Taphonomy and phytoliths: a user manual. Quat Int 275:76–83. https://doi.org/10.1016/j.quaint.2011.09.008

Madella M, Jones MK, Echlin P, Powers-Jones A, Moore M (2009) Plant water availability and analytical microscopy of phytoliths: implications for ancient irrigation in arid zones. Quat Int 193:32–40. https://doi.org/10.1016/j.quaint.2007.06.012

Manning K, Timpson A (2014) The demographic response to Holocene climate change in the Sahara. Quat Sci Rev 101:28–35. https://doi.org/10.1016/j.quascirev.2014.07.003

Manning K, Pelling R, Higham T, Schwenniger J-L, Fuller DQ (2011) 4500-Year old domesticated pearl millet (*Pennisetum glaucum*) from the Tilemsi Valley, Mali: new insights into an alternative cereal domestication pathway. J Archaeol Sci 38:312–322. https://doi.org/10.1016/j.jas.2010.09.007

Marshall F, Weissbrod L (2011) Domestication processes and morphological change: through the Lens of the Donkey and African Pastoralism. Curr Anthropol 52(Suppl):S397–S413. https://doi.org/10.1086/658389

Mateos-Naranjo E, Andrades-Moreno L, Davy AJ (2013) Silicon alleviates deleterious effects of high salinity on the halophytic grass *Spartina densiflora*. Plant Physiol Biochem 63:115–121. https://doi.org/10.1016/j.plaphy.2012.11.015

Mercader J, Astudillo F, Barkworth M et al (2010) Poaceae phytoliths from the Niassa Rift, Mozambique. J Archaeol Sci 37. https://doi.org/10.1016/j.jas.2010.03.001. 1,953–1,967

Meunier JD, Barboni D, Anwar-ul-Haq M et al (2017) Effect of phytoliths for mitigating water stress in durum wheat. New Phytol 215:229–239. https://doi.org/10.1111/nph.14554

Motomura H (2004) Silica deposition in relation to Ageing of Leaf tissues in Sasa veitchii (Carriere) Rehder (Poaceae: Bambusoideae). Ann Bot 93:235–248. https://doi.org/10.1093/aob/mch034

Nitsch EK, Charles M, Bogaard A (2015) Calculating a statistically robust $\delta^{13}C$ and $\delta^{15}N$ offset for charred cereal and pulse seeds. STAR: Sci Technol Archaeol Res 1:1–8. https://doi.org/10.1179/2054892315Y.0000000001

Oliva KME, da Silva FBV, Araújo PRM et al (2021) Amorphous silica-based fertilizer increases stalks and Sugar Yield and Resistance to stalk borer in sugarcane grown under field conditions. J Soil Sci Plant Nutr 21:2518–2529. https://doi.org/10.1007/s42729-021-00543-8

Olsen JT, Caudle KL, Johnson LC, Baer SG, Maricle BR (2013) Environmental and genetic variation in leaf anatomy among populations of *Andropogon gerardii* (Poaceae) along a precipitation gradient. Am J Bot 100:1957–1968. https://doi.org/10.3732/ajb.1200628

Out WA, Madella M (2017) Towards improved detection and identification of crop by-products: morphometric analysis of bilobate leaf phytoliths of *Pennisetum glaucum* and *Sorghum bicolor*. Quat Int 434:1–14. https://doi.org/10.1016/j.quaint.2015.07.017

Peduzzi PN, Hardy RJ, Holford TR (1980) A Stepwise Variable Selection Procedure for Nonlinear Regression models. Biometrics 36:511–516. https://doi.org/10.2307/2530219

Piperno DR (2006) Phytoliths: a Comprehensive Guide for archaeologists and paleoecologists. AltaMira, Oxford

Pokharia AK, Kharakwal JS, Srivastava A (2014) Archaeobotanical evidence of millets in the Indian subcontinent with some observations on their role in the Indus civilization. J Archaeol Sci 42:442–455. https://doi.org/10.1016/j.jas.2013.11.029

Portmann FT, Siebert S, Döll P (2010) Glob Biogeochem Cycles 24:GB1011. https://doi.org/10.1029/2008GB003435. MIRCA2000–Global monthly irrigated and rainfed crop areas around the year 2000: A new high-resolution data set for agricultural and hydrological modelling

Prinz D (2002) The role of water harvesting in alleviating water scarcity in arid areas. Keynote Lecture, Proceedings, International Conference on Water Resources Management in Arid Regions, 23–27 March, 2002, Kuwait Institute for Scientific Research, Kuwait, (Vol. III, 107–122)

Reynolds JF, Stafford Smith DM, Lambin EF et al (2007) Global desertification: building a science for Dryland Development. Science 316:847–851. https://doi.org/10.1126/science.1131634

Rodrigues FÁ, Vale FXR, Korndörfer GH et al (2003) Influence of silicon on sheath blight of rice in Brazil. Crop Prot 22:23–29. https://doi.org/10.1016/S0261-2194(02)00084-4

Rosen AM, Weiner S (1994) Identifying ancient irrigation: a New Method using Opaline Phytoliths from Emmer Wheat. J Archaeol Sci 21:125–132. https://doi.org/10.1006/jasc.1994.1013

Ruiz-Giralt A, Beldados A, Biagetti S et al (2023a) Sorghum and Finger Millet Cultivation during the Aksumite period: insights from Ethnoarchaeological Modelling and Microbotanical Analysis. J Comput Appl Archaeol 6:96–116. https://doi.org/10.5334/jcaa.132

Ruiz-Giralt A, Nixon-Darcus L, D'Andrea AC et al (2023b) On the verge of domestication: early use of C_4 plants in the Horn of Africa. Proc Natl Acad Sci USA 120:e2300166120. https://doi.org/10.1073/pnas.2300166120

Sage RF (2004) The evolution of C_4 photosynthesis. New Phytol 161:341–370. https://doi.org/10.1111/j.1469-8137.2004.00974.x

Sangster AG, Hodson MJ, Tubb HJ (2001) Chap. 5 Silicon deposition in higher plants. In: Datnof LE, Snyder GH, Korndörfer GH (eds) Silicon in Agriculture. Studies in Plant Science, vol 8. Elsevier, Amsterdam, pp 85–113

Schuster A-C, Burghardt M, Riederer M (2017) The ecophysiology of leaf cuticular transpiration: are cuticular water permeabilities adapted to ecological conditions? J Exp Bot 68:5:271–5279. https://doi.org/10.1093/jxb/erx321

Strömberg CAE (2009) Methodological concerns for analysis of phytolith assemblages: does count size matter? Quat Int 193:124–140. https://doi.org/10.1016/j.quaint.2007.11.008

Vadez V, Krishnamurthy L, Hash CT et al (2011) Yield, transpiration efficiency, and water-use variations and their interrelationships in the sorghum reference collection. Crop Pasture Sci 62:645–655. https://doi.org/10.1071/CP11007

Vadez V, Choudhary S, Kholová J et al (2021) Transpiration efficiency: insights from comparisons of C_4 cereal species. J Exp Bot 72:5221–5234. https://doi.org/10.1093/jxb/erab251

Varalli A, D'Agostini F, Madella M, Fiorentino G, Lancelotti C (2023) Charring effects on stable carbon and nitrogen isotope values on C_4 plants: inferences for archaeological investigations. J Archaeol Sci 156:105821. https://doi.org/10.1016/j.jas.2023.105821

Wang C, Lu H, Zhang J, Mao L, Ge Y (2019) Bulliform Phytolith size of Rice and its correlation with hydrothermal environment: a preliminary morphological study on species in Southern China. Front Plant Sci 10:1037. https://doi.org/10.3389/fpls.2019.01037

Weber SA, Fuller DQ (2008) Millets and their role in early agriculture. Pragdhara 18:69–90

Weber S, Kashyap A (2016) The vanishing millets of the Indus civilization. Archaeol Anthropol Sci 8:9–15. https://doi.org/10.1007/s12520-013-0143-6

Weisskopf A, Qin L, Ding J et al (2015) Phytoliths and rice: from wet to dry and back again in the Neolithic Lower Yangtze. Antiquity 89:1051–1063. https://doi.org/10.15184/aqy.2015.94

Winchell F, Brass M, Manzo A et al (2018) On the origins and Dissemination of Domesticated Sorghum and Pearl Millet across Africa and into India: a view from the Butana Group of the Far Eastern Sahel. Afr Archaeol Rev 35:483–505. https://doi.org/10.1007/s10437-018-9314-2

Winslow M, Shapiro BI, Thomas R, Shetty SVR (2004) Desertification, Drought, Poverty and Agriculture: Research Lessons and Opportunities. International Centre for Agriculture Research in the Dry Areas. http://www.iwmi.cgiar.org/Assessment/files/Synthesis/Land%20Degradation/DDPAARLO_text.pdf. Accessed 18 February 2009

Yang Q, Li X, Liu W et al (2011) Carbon isotope fractionation during low temperature carbonization of foxtail and common millets. Org Geochem 42:713–719. https://doi.org/10.1016/j.orggeochem.2011.06.012

Yoshida S, Ohnishi Y, Kitagishi K (1962) Histochemistry of Silicon in Rice Plant: III. The Presence of cuticle-silica double layer in the epidermal tissue. Soil Sci Plant Nutr 8:1–5. https://doi.org/10.1080/00380768.1962.10430982

Zaman-Allah M, Jenkinson DM, Vadez V (2011) A conservative pattern of water use, rather than deep or profuse rooting, is critical for the terminal drought tolerance of chickpea. J Exp Bot 62:4239–4252. https://doi.org/10.1093/jxb/err139

Zurro D (2018) One, two, three phytoliths: assessing the minimum phytolith sum for archaeological studies. Archaeol Anthropol Sci 10. https://doi.org/10.1007/s12520-017-0479-4. 1,673–1,691